Investigation of drug distribution in tablets using surface enhanced Raman chemical imaging

Journal of Pharmaceutical and Biomedical Analysis, 76 (2013) 145-151
DOI: 10.1016/j.jpba.2012.12.017

*Graphical Abstract

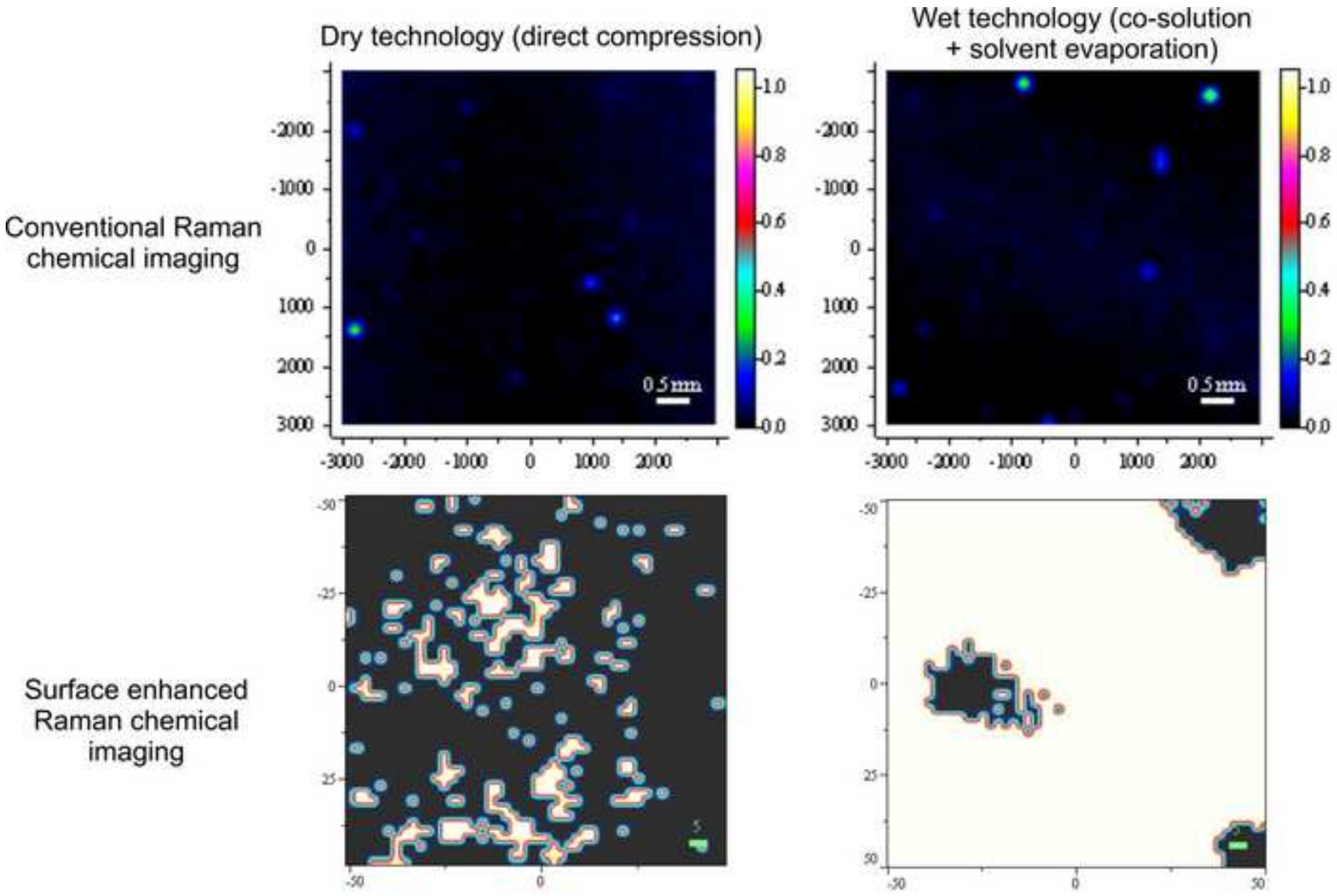

Highlights

1. Raman chemical imaging was enhanced by applying SERS colloid on the samples.
2. Distribution of trace amount of API was revealed below Raman limit of detection.
3. Asymmetric least squares, a new method was used for baseline correction.
4. MCR-ALS is required to resolve and identify SERS spectra and to create images.
5. Proposed method intended for comparison of unknown samples with trace amount of drug.

Investigation of drug distribution in tablets using surface enhanced Raman chemical imaging

Tamás Firkala[a], Attila Farkas[b], Balázs Vajna[b,*], István Farkas[b], György Marosi[b]

[a] Institute of Materials and Environmental Chemistry, Research Centre for Natural Sciences, Hungarian Academy of Sciences, 1025 Budapest, Pusztaszeri út 59-67, Hungary

[b] Department of Organic Chemistry and Technology, Budapest University of Technology and Economics, H-1111 Budapest, Budafoki út 8., Hungary

* Corresponding author:
Tel.: +353 87 067 7050
E-mail: balazs.vajna@gmail.com

Abstract

This paper reports the first application of surface enhanced Raman chemical imaging on pharmaceutical tablets containing the active ingredient (API) in very low concentrations. Taking advantage of the extremely intensive Raman signals in the presence of silver colloids, image aquisition time was radically decreased. Moreover, the investigation of drug distribution below the detection limit of regular micro-Raman spectrometry was made

feasible. The characteristics of different manufacturing technologies could be revealed at very low API concentrations by using chemometric methods for processing and evaluating the large number of varying spectra provided with this imaging method.

1. Introduction

Surface-enhanced Raman spectroscopy (SERS), based on the phenomenon known as surface enhanced Raman scattering, has been gaining particular attention in pharmaeutical research in the recent years [1-3]. Using this technique, the presence of certain compounds (having appropriate molecular structure) can be detected at extremely low concentrations [4,5] and this feature makes Raman spectroscopy capable of analyzing trace amounts of such analytes. Therefore the technique has become very important in pharmaceutical and biological analysis, while applications in other fields are continuously expanding as well [6,7].

In spite of the rapid expansion of the application of SERS technique, its combination with Raman chemial imaging (R-CI) has just come into focus in the recent years [8-13]. This combination results in a special imaging method which is based on the selective detection of SERS active points of the scanned surface. Surface enhanced Raman chemical imaging (SER-CI) has been successfully applied in certain territories of biomedical science, such as cell investigations [10] or bacterial mixture identification [11]. SER-CI has also been combined with atomic force microscopy resulting in a promising imaging technique called tip enhanced Raman spectroscopy [12] which has been shown to have great potential in semiconductor technologies [13].

The fight against illegal and counterfeit products is a continuously growing issue of high importance nowadays on the pharmaceutical and black markets [14-16]. Work has been started recently to find the advantages of SERS in the investigation of pharmaceutical and

illegal tablets [17]. The potential of its combination with chemical imaging of tablets (their outer or broken surface), however, has not yet been explored in either the field of pharmaceutical technology, or in forensic applications (to the authors best knowledge).

While the non-imaging SERS technique focuses only on the *detection* of an active ingredient (or a similar compound such as an illegal drug), one of the most promising application of SER-CI is the spatial mapping of drug distribution in the investigated tablets. One of the main goals of R-CI in pharmaceutical technology is to understand the characteristics of drug dissolution and other physicochemical features by determining the distribution of constituents within a tablet. In the course of forensic identification of illegal tablets, the same analysis can lead to the determination of the manufacturing technology or the comparison of multiple tablets to see if they had been manufactured with the same technology (i.e. possibly at the same location or lab). In the latter case, however, two problems arise: one is that the components of an illegal tablet are usually unknown; the other is that drugs are often present in very low overall concentrations. Although it can be possible to detect very low concentrations (0,025-0,1% w/w) with normal RCI as well [18,19], this is only possible if the drug, although globally present in very low concentrations, can be locally detected in the form of distinct particles. Even in such a case the other main problem is the unavoidably high overall image acquisition time due to the high number of required measurement points (pixels) and the high acquisition time to reach appropriate signal-to-noise ratio. Where the trace drug is distributed homogeneously, conventional R-CI does not offer any advantages to the bulk analysis of tablets (e.g. with non-imaging Raman or NIR spectroscopy).

The present paper offers a solution to the problem of determining the spatial distribution of a trace active ingredient by combining R-CI with the SERS technique and with chemometric evaluation using multivariate curve resolution algorithms.

2. Materials and methods:

2.1. Preparation of tablets

Lactose monohydrate (LMH) and trisodium citrate was purchased from Sigma Aldrich Corporation. Acetylsalycilic acid (further referred to as API i.e. the active pharmaceutical ingredient), was manufactured by Richter Gedeon Plc (Hungary). Dimethyl-sulfoxide and silver-nitrate were purchased from Reanal Ltd (Hungary).

„Dry technology" (D) tablets with heterogeneous drug distribution were prepared by thorough blending of API and LMH using a mortar and pestle. In order to achieve homogeneous distribution in „wet technology" (W) tablets, 2 g API-LMH blend was dissolved in 10 ml dimethyl sulfoxide and then the solvent was evaporated with vacuum distillation.

API:LMH mass ratio was 1:399 in both tablet batches (i.e. tablets had 0.25% API in mass fractions). Model tablets, each weighting 400 mg, were prepared in a Manfredi 0057C00 type KBr disk press (Italy).

2.2. Preparation of SERS colloids

Ag nanoparticles were prepared by Lee and Meisel's method [20], widely used to synthesize silver for SERS substrates [21-25]. Silver-nitrate of 0,09g was dissolved in 0,5l of double distilled water. The solution was heated to boil and 10ml of 1% trisodium-citrate aqueous solution was added *dropwise* into to boiling solution during vigorous stirring. Boiling was continued for 10 more minutes. Finally a greenish-grey colloidal solution was obtained.

Before SER-CI measurements the suspension was concentrated, via centrifugation, by a factor of 10.

2.3. Raman instrumentation:

Raman mapping spectra were collected using a LabRAM system (Horiba Jobin-Yvon, Lyon, France) coupled with an external 532 nm Nd-YAG laser source (Sacher Lasertechnik, Marburg, Germany) and an Olympus BX-40 optical microscope (Olympus, Hamburg, Germany). An objective of 50× magnification was used for optical imaging and spectrum acquisition. The laser beam, after an optional intensity filter, is directed through the objective, and backscattered radiation is collected with the same objective. The collected radiation is directed through a notch filter that removes the Rayleigh photons, then through a confocal hole (1000 μm) and an entrance slit (100 μm) onto a grating monochromator (1800 grooves/mm) that disperses the light before it reaches the CCD detector. The spectrograph was set to provide a spectral range of 550–1750 cm^{-1} and 3 cm^{-1} resolution.

The outer surface of tablets were investigated (without any sample preparation) in each mapping experiment. Prior to SER-CI analysis, two types of reference maps had been taken from the tablets. The first type („background") reference used exactly same imaging acquisition conditions as SER-CI analyses (see later) to ensure that no signals of the API (or the excipient) are detected without SERS. Such ("background") maps, as they indeed consisted of noise only, are not shown in the paper.

The second type of reference (R-CI) images were obtained with'traditional' Raman imaging conditions, setting high enough acquisition time to see the signals of the ingredients and attempt to reveal the distribution of the trace API without SERS. To achieve this, spectrum acquisition time was 3 s and 20 such spectra were accumulated and averaged at each

pixel to achieve acceptable signal-to-noise ratio. The step size between adjacent pixels was increased to 200 μm along both axes in order to utilize the high overall measurement time and to increase the probability of finding pixels that contain the API. As a compromise between image size and overall mapping acquisition time, the measured area on the tablet surfaces was 31×31 pixels and acquisition of each of these maps took over 14 hours.

For SER-CI analysis SERS colloid solution was dripped on top of the tablets and, after drying, mapping was carried out on their outer surface (i.e. without any further sample preparation to avoid alteration of the sample structure). Spectrum acquisition time in this case was 0,5 s per pixel and only 1 spectrum was measured at each point without multiple accumulation or averaging, to avoid degradation of the silver colloids. In this case, a step size of 2μm was used between adjacent pixels to achieve high spatial resolution, and the investigated area was at least 49×49 pixels. The overall acquisition time for each SER-CI and „background" image (without SERS) was 20 min. For SER-CI analysis the laser power was reduced to 10% of its original value with an intensity filter for the same purpose (to avoid damage to colloids), while full power (~50 mW) was applied for the conventional R-CI investigations.

To compensate the small measured area with SER-CI maps due to the low step size, three separate SER-CI maps were collected from different locations on each tablet. Multiple tablets were investigated to verify reproducibility but only one tablet of each batch is discussed in detail.

2.4. Data analysis

Before chemometric evaluation, all spectra were base-line corrected using Eiler's asymmetric least squares method [26] with parameters of $\lambda=10^5$ and $p=10^{-3}$. For comparison, the traditional approach of piece-wise linear baseline correction was also tested with manually selected baseline points. The measured spectra were then normalized to unit area in order to eliminate the intensity deviation among the measured points. The raw three-dimensional data was unfolded into a 2-dimensional matrix (for the procedure, see reference [14]).

The estimation of pure component spectra from the Raman maps was carried out by multivariate curve resolution – alternating least squares (MCR-ALS [27,28]). This technique is based on the following bilinear model:

$$\mathbf{X} = \mathbf{C}\mathbf{S}^T + \mathbf{E} \qquad \text{(Eq. 1)}$$

$\mathbf{S}^T$ ($k \times \lambda$) is the set of reference (pure component) spectra, $\mathbf{X}$ ($p \times \lambda$) is the matrix containing the mapping spectra, and $\mathbf{C}$ ($p \times k$) contains the vectors of spectral concentrations (each row in $\mathbf{C}$ contains the concentrations of the k ingredients). The matrix $\mathbf{E}$ represents the residual noise. If the spectra of the pure components are known, the $\mathbf{C}$ matrix can be calculated in a straightforward way with the Classical Least Squares (CLS) calculation, using $\mathbf{X}$ and $\mathbf{S}^T$. This is comprehensively described in numerous papers [14-16]. If some or all of the components are unknown, MCR-ALS can be used, which itself generates both the concentration (also known as *score*) matrix $\mathbf{C}$ and pure spectrum (also known as *loading*) matrix $\mathbf{S}^T$ from the dataset $\mathbf{X}$ in an iterative manner, using an initial estimation for either $\mathbf{C}$ or $\mathbf{S}^T$ and appropriate physical constraints. Easy to use programs are available from the developers [27] and in commercial software [29]. All of these have internal algorithms for providing the initial estimations and the iterations afterwards, and require minimal effort from the user. Only non-negativity constraints were used in our study.

The resolved loadings (i.e. estimated pure component spectra) were inspected one by one and only those loadings were chosen for further use, which carried specific (sharp)

vibrational peaks. The approach proposed here assumes that only the API is SERS active. (The rest of the loadings contained noise spikes and other disturbance factors arising due to the partial degreadation of SERS colloids in some of the pixels.) The scores corresponding to these loadings were set in descending order and a threshold was determined for each API spectrum. Those values were chosen as thresholds, which showed dominant change in API peak intensity. Pixels with an API score over this threshold were assigned the value of '1', i.e. to the API, while the rest were given a '0' value. This classification was accomplished using a Visual Basic algorithm written in-house. Then the received column vector of these binarized scores was formed back into an image matrix by using the *reshape* command in Matlab.

In the case of R-CI investigations, MCR-ALS scores (i.e. spectral concentrations) were directly used to produce spatial distribution images, as usually done in most R-CI investigations [14-16, 30-34]. R-CI score images obtained by multivariate techniques usually do not require binarization to highlight the presence of an active ingredient, and the scores can be interpreted as estimated concentrations (unlike in the case of SER-CI where only the signal coming from SERS-active components are used and the raw scores do not hold information about the actual concentration). Preliminary studies with and without binarization yielded images with the same number of API-positive pixels, hence it was regarded as an unnecessary step for R-CI.

All calculations were performed in MATLAB 7.6.0 (Mathworks, USA) with PLS_Toolbox 6.2 and MIA_Toolbox 2.5 (Eigenvector Research, USA). Other curve resolution and factor analysis methods are also available, but only MCR-ALS was used as numerous studies have proven it to be the best choice for this purpose [30-34].

Spectral concentrations of the ingredients present in the sample (further also referred to as 'Raman scores' in order to avoid confusion with real concentrations) were computed with the same algorithm described above.

Visualization of spectra and spatial distribution maps was carried out with LabSpec 5.41 (Horiba Jobin Yvon, France). The statistical properties of scores (mean, standard deviation) were computed with MATLAB.

3. Results and discussion

In order to demonstrate how SERS can enable the detection of traces of active ingredients in a solid product and the determination of their spatial distribution with R-CI special attention had to be paid to the selection of a suitable chemometric method . As SERS spectra usually have significant differences from the regular Raman spectrum of the same substance, the usual preprocessing methods and the conventional evaluation of images with classical least squares (CLS) are not feasible. Furthermore, Raman images tend to consist of a huge amount of measured spectra (a few thousands in our case). Therefore, a new way of evaluation, based on currently available chemometric methods, had to be developed. This study uses multivariate curve resolution – alternating least squares (MCR-ALS) for this purpose, which have already been proven to be the most efficient in the evaluation of Raman maps [30-34].

3.1. R-CI investigations without SERS

Conventional R-CI maps of (both known and unknown) pharmaceuticals can be evaluated in a straightforward manner by resolving an appropriate number of spectra using MCR-ALS. (CLS with the pure reference spectra would usually also be an option in the pharmaceutical practice, but not in forensics and when unknown samples are investigated.)

Figure 1 shows the spectra resolved using MCR-ALS decomposition. In order to properly estimate the number of components present in the sample, the number of spectra to be resolved has to be overestimated. Due to this overestimation, the outcome contains certain loadings, the features of which are very similar to one another and which in fact correspond to the same physicochemical component. If these small differences can be explained or are irrelevant with respect to the results, these similar loadings can be averaged to get a more accurate estimation of the pure component spectra [34]. Note in this case the number of components is known, so it would have been possible to resolve just two spectra, but the study follows the practice of investigating an unknown tablet as proposed in the literature. [33, 34])

Figure 1.

The spectra of ’D’ (dry technology) tablet, resolved by initializing MCR-ALS with 6 pseudorandom vectors, are shown in Fig. 1a. The first loading clearly belongs to API, while all the others are corresponding to the LMH. The differences among the LMH loadings are caused by polarization effects which introduce remarkable deviation in the relative intensities of certain peaks (e.g. 1084 and 851 cm^{-1}). Note the peak positions are same and there is no band widening or shape alteration which would indicate different molecular or solid state structures. Lactose is known to be generally sensitive to the polarization of the laser light, while other substances show little intensity deviations owing to this phenomenon. This effect is more apparent in microscopic spectrometry, and usually occurs at high magnifications where the crystal size is larger than the irradiated sample volume. Figure 1b shows the resolved spectra of ’W’ (wet technology) tablet.

Figure 2 shows the spatial distribution of the API based on the MCR-ALS scores (concentrations) corresponding to the first loading. Figure 2a shows large dark areas in the map of the ’D’ tablet that do not contain any API. In several points, however, a low amount of API can be detected. The distribution image of the ’W’ tablet (Fig. 2b) is very similar to the one of the ’D’ tablet, thus, the two technologies cannot be distinguished by R-CI at such low API concentration. The question remains whether the dark areas are truly free of the active ingredient or it is actually present under the R-CI limit of detection.

Figure 2.

3.2. Evaluation of SER-CI images

The evaluation of SER-CI experiments is challenged by two main phenomena. On one hand, the spectra recorded with very short exposure time (0.5 sec) and aquisition number have a low signal-noise ratio. This has only minor effect on the evaluation, as noise is usually averaged out when the entire dataset of hundreds/thousands of spectra is processed with chemometric tools. On the other hand, SERS spectra of the same component show very high variability when microscopic imaging is used. aspirin molecules bound to silver nanoparticles can be polarized in various ways, since the shapes and sizes of silver nanoparticles prepared with Lee and Meisel’s method are not exactly uniform [35]. (It is generally well known that the SERS effect investigated in a colloid system has particle size and particle shape dependence [17,36,37].) When samples are analyzed in a solution, using a macroscopic (non-imaging) spectrometer, an average spectrum is obtained, simultaneously collecting signals from variously polarized analyte molecules. On the surface of dry samples, however, SERS

particles are immobilized and, in chemical imaging, only a small area is investigated at once, therefore no averaging occurs and the pixel-by-pixel high variablility among the SERS spectra is revealed. This results in an extreme deviation in the position, intensity and shapes of the surface-enhanced Raman-bands of the API. Due to the presence of SERS colloids, the baseline is also perturbed and varies significantly among the pixels. Consequently, neither the CLS method (using pre-defined reference spectra), nor the univariate approach with a selected peak can be used in practice to accurately determine the presence of the API via its SERS signals. Furthermore, an appropriate solution had to be found for the baseline correction as well.

3.2.1. A suitable preprocessing method for SERS spectra

To remove of fluorescent background from the SER-CI datasets, asymmetric least squares was used, originally developed by Eilers for preprocessing chromatograms [38]. Asymmetric least squares (not to be confused with alternating least squares in curve resolution) is derived from the Whitaker smoother [39], and is a fast and more efficient alternative to the widely popular Savitzky-Golay [40] filter. The details are comprehensibly described by its developer [26].

Figure 3.

Although this had been originally developed as a flexible smoothing tool, it can be just as well used to estimate a nonlinear background by „oversmoothing” peaks. The main advantage of this approach is that no wavenumbers have to be pre-selected to fit a (linear or nonlinear) curve to estimate the background, hence it is resistant to the variablility of peak

297 shapes and positions and to the emergence of unexpected SERS bands. Its comparison with
298 piece-wise baseline correction is depicted on Figure 3. The quality of the baseline depends
299 slightly on the asymmetric parameter (p) and mainly on the smoothing parameter (λ).
300 Oversmoothing is generally carried out by using a very high ($>10^4$) λ value. After testing
301 numerous combinations, their best values were determined as p = 0.001 and $\lambda = 10^5$. When
302 the parameters are optimized and fixed, the baseline itself has to be separately calculated for
303 each mapping spectrum. A Matlab algorithm, relying on Eiler's algorithmic functions, is
304 provided in the Appendix in the electronic supplementary material to create a baseline-
305 corrected matrix from the input dataset. Afterwards, the same usual further steps (e.g.
306 normalization) can be applied as in R-CI investigations.
307
308
309 3.2.2. Evaluation of resolved spectra
310
311 Appropriate preprocessing is only the first step in overcoming the challenges of SER-
312 CI. The other problem is that the variability in the SERS spectrum of the API has to be taken
313 into consideration in the modelling. MCR-ALS curve resolution was therefore performed with
314 an approriately high number of resolved loadings (in this case 20) to separate all independent
315 signals from each other. The identification of these loadings was performed visually by
316 determining whether sharp vibrational peaks are present, assuming that they originate from
317 the API (which was true in this case, as lactose is not SERS active). It was found that only a
318 few loadings carried typical bands belonging to the API, while others almost completely
319 consisted of noise and interfering signals from the silver colloid. All loadings are shown in
320 Figure SM-1 ("D" tablet) and SM-2 ("W" tablet) in the supplementary material, whereas

those corresponding to the API are summarized in Figure 4. Interfering signals from the colloid are illustrated on Figure SM-3 in the supplementary material.

The loadings identified as Aspirin SERS spectra were compared with the pure acetyl-salycilic acid spectrum on the Figure 4. The selected spectra were the loadings 5, 7 and 14 in the case of ’D’ tablet. Similarly, three loadings contained features similar to the pure API spectra (namely loadings 1, 7 and 8) for the “W” tablet. It has to be noted, that the number of the API-related loadings varied in the reproducted experiments. It can be also seen that in different SERS spectra different bands are enhanced and to various extent: in many cases, the intensities of such bands are amplified which are otherwise very weak in the conventional Raman spectrum of the API. This is why neither a univariate approach nor CLS modelling with reference spectra can be applied to evaluate the maps – instead, curve resolution algorithms (such as MCR-ALS) are needed, which can detect each spectrum that has different peak structures. Setting a high number of loadings to resolve is important to capture as many different API-related loadings as possible. (It has to be noted that using SERS colloids of uniform shape and narrow size range would most probably result in more uniform SERS spectra and a lower number of distinct API-related loadings, however, this would not provide any particular benefit for the chemometric evaluation proposed here. Using appropriate baseline correction with asymmetric least squares and data decomposition with MCR-ALS allows the use of less expensive SERS colloids or those prepared in-house, thereby notably increasing cost efficiency.)

Figure 4.

3.2.3. Visualization of surface-enhanced distribution maps

Along with the loadings the score vectors were also calculated, which are usually used as estimations of the concentration. In this case, they are used for determining whether an API SERS signal was detected in a pixel or not. For each SERS loading, this was carried out by sorting these score values by magnitude and finding a threshold above which the corresponding loading is identified as significantly being present. The threshold, separately for each loading, can be easily determined visually by sequentially bisectioning ("halving") the sorted scores, and checking the corresponding spectrum on the map, in a few steps. The method is the following: (1) Take the score in the middle of the sorted score list. (2) Visually check the mapping spectrum having this score value. (3) If this spectrum has visible SERS (in this case, API) peaks, then proceed to the lower half of sorted scores and repeat the process from step (1). Otherwise, proceed to the upper half of the sorted scores and repeat from step (1). A good threshold is quickly received in n steps for a map containing up to 2^n pixels. After determining the score threshold for each API-related loading, all scores can be binarized based on whether they are higher (1 or "SERS-positive") or lower (0 or "SERS-negative") than the threshold and the pixels with SERS signals present can be counted on the Raman map.

The binarized scores, each indicating if the API was detected via its SERS signal in a pixel, can be refolded to a spatial image in the same way the concentration images are usually produced. As the investigated area of a SER-CI map (60 μm × 60 μm) was smaller than the area covered by an R-CI reference map (200 μm × 200 μm), three SER-CI maps were acquired from different, randomly selected locations from both "D" and "W" tablets. This was done to ensure that different locations show the same characteristics with regards to the API distribution. Figure 5 proves that in contrast to conventional R-CI, the difference between

the dry and wet technologies can be easily recognized based on the SER-CI maps. These findings are supported by Table 1 highlighting the number of pixels with the API present. While the API was detected in a relatively small number of distinct pixels in the ’D’ tablet (9-14%), in the case of ’W’ tablets the SERS signals of aspirin were detected in the vast majority of the pixels (91-98%).

Table 1 shows that the number of SERS-positive pixels were consequently 8-10× more in the ’W’ tablets than in the ’D’ tablets, unambigously differentiating the wet and dry manufacturing technologies. This means that when the tablet is prepared by wet granulation, the API forms a narrow layer on the excipient particles, which cannot be detected with R-CI if the overall concentration of API is very low (0.25% in this case), but can be unambiguously detected if SERS colloid is applied on the tablet surface.

Figure 5.

Table 1.

The traditional R-CI concentration maps, obtained with much longer measurement time, were plotted on the Figure 2, where the two manufacturing technologies could not be distinguished. The reason is that the API is under the limit of detection in the majority of pixels in the map of the W tablet. If silver colloids are used to enhance the API spectra, the presence of API is revealed in more than 90% of pixels for the “W” tablet, where a fraction of the API is homogeneously distributed throughout the whole tablet due to the wet technology. This is ten times more than the number SERS-positive pixels spectra when the tablet was prepared with a dry technology (comparing maps of approximately the same sizes). Much fewer API-positive pixels are detected by R-CI investigations, in which case the difference –

without lingering reproducibility studies – is not drastic enough to unambiguously differentiate between the two technologies. Besides, such reproducibility studies are often impossible in real-life forensic studies where only one or very few samples are available for investigation.

Another advantage of the SER-CI method is the outstanding decrease of mapping acquisition time, while using the same instrumental set-up as for ordinary R-CI studies. While each R-CI measurement took over 14 hours, the overall acquisition time for a SER-CI map – with a higher number of pixels – took only 20 minutes. Even the acquisition of multiple SER-CI maps will be significantly less time-consuming than ordinary R-CI, while delivering more information.

It has to be noted that the model tablets in this case contained the API in the same concentration (0.25%). Some studies tend to correlate the percentage of pixels with a certain component present (i.e. the surface coverage of that component) with the overall concentration of that component in the sample [41]. It has been already shown for ordinary R-CI that the surface coverage and the estimated overall concentrations depend on the manufacturing technology [42], this phenomenon is extremely amplified when SERS is used, and the maps currently cannot be processed to provide (semi-)quantitative information about the API content. Therefore further studies are required to develop a semi-quantitative method to estimate the amount of the active ingredient using SER-CI. Another drawback of the currently proposed evaluation approach to SER-CI maps is that it does not offer an automated method to determine if the SERS signals are arising from one component only or there are multiple, physicochemically different components simultaneously showing SERS spectra. As already the SERS spectra of the same component show lot of variation among pixels, further studies are needed to determine if multiple SERS-active components can be distinguished

based on their resolved loadings, to separately plot their surface coverage on the visualized images.

4. Conclusions

Surface enhanced chemical imaging was reported for the first time to investigate and compare drug containing tablets with trace amounts of active ingredient. The method was found suitable in the determination of the manufacturing technology even in cases where ordinary Raman mapping (without SERS) does not show any significant difference between tablets prepared with different manufacturing technologies. This broadens the opportunities to determine if multiple unknown (possibly illegal) tablets containing trace amounts of drug have been manufactured by the same or different technologies (i.e. presumably in the same location or different ones). In the present study, tablets produced with a dry (direct compression) and a wet technology (co-solution and solvent evaporation, then compression) were investigated. Combining SERS with chemical imaging enabled the detection of the active ingredient in areas where its concentration level was well below the Raman spectrometric limit of detection, thus revealing its true spatial distribution in the tablets. Furthermore, by enhancing API signals via SERS, generally a 120-fold reduction was achieved in the image aquisition time. This, of course, is only possible if the active ingredient is SERS active (and the current evaluation assumes that only one ingredient, i.e. the drug, is SERS active).

Surface enhanced Raman chemical maps pose a great challenge to evaluate, due to the high variability of spectra arising from the colloid size and shape dependence of the SERS signals. When microscopic imaging of a solid sample is performed, these variances are not

averaged out as they otherwise do for bulk spectroscopic measurements. A new approach was hence developed by using asymmetric least squares preprocessing with appropriately chosen parameters to enable background estimation, followed by MCR-ALS data decomposition to find all the various SERS positive (in this case, API-related) loadings.

The present study is the first step in the combined application of SERS, Raman chemical imaging, appropriate data preprocessing and chemometric evaluation in the structural characterization of tablets with trace amounts of drugs present. The proposed evaluation approach is intended to be applicable for such tablets where no prior information is available about the ingredients. SER-CI poses lots of challenges, some of which were solved here and some have to be overcome in the future, but may become a powerful tool in the investigation of unknown (possibly illegal) products.

Acknowledgements

The authors would like to express their thanks to Dr. Ferenc Somodi for his help in the experiments of SERS substrate preparation. The research was supported by the ERA Chemistry (code NN 82426) and W2Plastics EU7 (code 212782) international projects and the Hungarian project TAMOP-4.2.1/B-09/1/KMR-2010-0002.

References

[1] M.H. Harpster, H. Zhang, A.K. Sankara-Warrier, B.H. Ray, T. R. Ward, J.P. Kollmar, K.T. Carron, J.O. Mecham, R.C. Corcoran, W.C. Wilson, P.A. Johnson, SERS detection of indirect viral DNA capture using colloidal gold and methylene blue as a Raman label, Biosens. Bioelectron. 25 (2009) 674-681.

[2] I-Hsien Chou, M. Benford, H.T. Beier, G.L. Coté, Nanofluidic Biosensing for β-Amyloid Detection Using Surface Enhanced Raman Spectroscopy, Nano Lett. 8 (2008) 1729-1735.

[3] K.C. Bantz, A.F. Meyer, N.J. Wittenberg, H. Im, Ö. Kurtulus, S.H. Lee, N.C. Lindquist, S. Oh, C.L. Haynes, Recent progress in SERS biosensing, Phys. Chem. Chem. Phys. 13 (2011) 11551-11567.

[4] P.G. Etchegoin, E.C. Le Ru, A perspective on single molecule SERS: current status and future challenges,
Phys. Chem. Chem. Phys. 10 (2008) 6079-6089.

[5] J. Jiang, K. Bosnick, M. Maillard, L. Brus, Single Molecule Raman Spectroscopy at the Junctions of Large Ag Nanocrystals, J. Phys. Chem. B 107 (2003), 9964-9972.

[6] S.I. Rae, I. Khan, Surface enhanced Raman spectroscopy (SERS) sensors for gas analysis, Analyst 135 (2010) 1365-1369.

[7] J. Du, C. Jing, Preparation of Fe_3O_4@Ag SERS substrate and its application in environmental Cr(VI) analysis, J. Colloid Interface Sci. 358 (2011) 54-61.

[8] S.P. Ravindranath, K.L. Henne, D.K. Thompson, J. Irudayaraj, Surface-Enhanced Raman Imaging of Intracellular Bioreduction of Chromate in Shewanella oneidensis, Plos One 6 (2011) 16634e.

[9] M. Lee, S Lee, J. Lee, H. Lim, G. Seong, E.K. Lee, S. Chang, C.H. Oh, J. Choo, Highly reproducible immunoassay of cancer markers on a gold-patterned microarray chip using surface-enhanced Raman scattering imaging, Biosens. Bioelectron. 26 (2011) 2135-2141.

[10] H. Park, S. Lee, L. Chen, E.K. Lee, S.Y. Shin, Y.H. Lee, S. W. Son, C.H. Oh, J.M. Song, S.H. Kang, J. Choo, SERS imaging of HER2-overexpressed MCF7 cells using antibody-conjugated gold nanorods, Phys. Chem. Chem. Phys, 11 (2009) 7444-7449.

[11] J. Guichetau, S. Christesen, D. Emge, A. Tripathi, Bacterial mixture identification using Raman and surface-enhanced Raman chemical imaging, J. Raman Spectrosc. 41 (2010),1632-1637.

[12] M. Chaigneau, G. Picardi, R. Ossikovski, Tip enhanced Raman spectroscopy evidence for amorphous carbon contamination on gold surfaces, Surf. Sci. 604 (2010) 701-705.

[13] N. Lee, R.D. Hartschuh, D. Mehtani, A. Kisliuk, J.F. Maguire, M. Green, M.D. Foster, A.P. Sokolov, High contrast scanning nano-Raman spectroscopy of silicon, J. Raman Spectrosc. 38 (2007) 789-796.

[14] C. Gendrin, Y. Roggo, C. Collet, Pharmaceutical applications of vibrational chemical imaging and chemometrics: A review, J. Pharm. Biomed. Anal. 48 (2008) 533-553.

[15] A.A. Gowen, C.P. O'Donnell, P.J. Cullen, S.E.J. Bell,Recent applications of Chemical Imaging to pharmaceutical process monitoring and quality control, Eur. J. Pharm. Biopharm. 69 (2008) 10-22.

[16] J.M. Amigo, Practical issues of hyperspectral imaging analysis of solid dosage forms, Anal. Bioanal. Chem. 398 (2010) 93-109.

[17] S.E.J. Bell, L.A. Fido, N.M.S. Sirimuthu, S.J. Speers, K.L. Peters, S.H. Cosbey, Screening tablets for DOB using surface-enhanced Raman spectroscopy, J. Forensic Sci. 52 (2007) 1063-1067.

[18] S. Šašić, M. Whitlock, Raman Mapping of Low-Content Active-Ingredient Pharmaceutical Formulations. Part II: Statistically Optimized Sampling for Detection of Less Than 1% of an Active Pharmaceutical Ingredient, Appl. Spectrosc. 62 (2008) 916-921.

519 [19] S. Šašić, S. Mehrens, Raman Chemical Mapping of Low-Content Active Pharmaceutical
520 Ingredient Formulations. III. Statistically Optimized Sampling and Detection of Polymorphic
521 Forms in Tablets on Stability, Anal. Chem. 84 (2012) 1019-1025.
522 [20] P.C. Lee , D. Meisel, Adsorption and surface-enhanced Raman of dyes on silver and gold
523 sols, J. Phys. Chem. 86 (1982) 3391- 3395.
524 [21] L. Ding, Y. Fang, An investigation of the surface-enhanced Raman scattering (SERS)
525 effect from laser irradiation of Ag nanoparticles prepared by trisodium citrate reduction
526 method, Appl. Surf. Sci. 253 (2007) 4450-4455.
527 [22] S.E.J. Bell and N.M.S. Sirimuthu, Surface-enhanced Raman spectroscopy as a probe of
528 competitive binding by anions to citrate-reduced silver colloids. J. Phys. Chem. A (109)
529 (2005) 7405-7410.
530 [23] L. Rivas, S. Sanchez-Cortes, J.V. Garcia-Ramos, and G. Morcillo, Growth of Silver
531 Colloidal Particles Obtained by Citrate Reduction To Increase the Raman Enhancement
532 Factor, Langmuir 17 (2001) 574-577.
533 [24] C.H. Munro, W.E. Smith, M. Garner, J. Clarkson, P.C. White, Characterization of the
534 Surface of a Citrate-Reduced Colloid Optimized for Use as a Substrate for Surface-Enhanced
535 Resonance Raman Scattering, Langmuir 11 (1995) 3712-3720.
536 [25] W. Ke, D. Zhou, J. Wu, K. Ji, Surface-Enhanced Raman Spectra of Calf Thymus DNA
537 Adsorbed on Concentrated Silver Colloid, Appl. Spectrosc. 59 (2005) 418-423.
538 [26] P. Eilers, A perfect smoother, Anal. Chem. 75 (2003) 3631-3636.
539 [27] J. Jaumot, R. Gargallo, A. de Juan, R. Tauler, A graphical user-friendly interface for
540 MCR-ALS: a new tool for multivariate curve resolution in MATLAB, Chemom. Intell. Lab.
541 Syst. 76 (2005) 101-110.
542 [28] R. Tauler, Multivariate curve resolution applied to second order data, Chemom. Intell.
543 Lab. Syst. 30 (1995) 133-146.

544 [29] B.M. Wise, N.B. Gallagher, Chemometrics Tutorial, Eigenvector Research Inc (2006)
545 [30] L. Duponchel, W. Elmi-Rayaleh, C. Ruckebusch, J.P. Huvenne, Multivariate curve
546 resolution methods in imaging spectroscopy: influence of extraction methods and
547 instrumental perturbations, J. Chem. Inf. Comput. Sci. 43 (2003) 2057-2067.
548 [31] C. Gendrin, Y. Roggo, C. Collet, Self-modelling curve resolution of near infrared
549 imaging data, J. Near Infrared Spectrosc. 16 (2008) 151-157.
550 [32] L. Zhang, M.J. Henson, S.S. Sekulic, Multivariate data analysis for Raman imaging of a
551 model pharmaceutical tablet, Anal. Chim. Acta 545 (2005) 262-278.
552 [33] B. Vajna, G. Patyi, Zs. Nagy, A. Farkas, Gy. Marosi, Comparison of chemometric
553 methods in the analysis of pharmaceuticals with hyperspectral Raman imaging, J. Raman
554 Spectrosc. 42 (2011) 1977-1986.
555 [34] B. Vajna, A. Farkas, H. Pataki, Zs. Zsigmond, T. Igricz, Gy. Marosi, Testing the
556 performance of pure spectrum resolution from Raman hyperspectral images of differently
557 manufactured pharmaceutical tablets, Anal. Chim. Acta. 712 (2012) 45-55.
558 [35] M. Rycenga, C.M. Cobley, J. Zeng, W. Li, C. H. Moran, Q. Zhang, D. Qin, Y. Xia,
559 Controlling the Synthesis and Assembly of Silver Nanostructures for Plasmonic Applications,
560 Chem. Rev. 111 (2011) 3669-3712.
561 [36] R.A. Alvarez-Puebla, R.F. Aroca, Synthesis of Silver Nanoparticles with Controllable
562 Surface Charge and Their Application to Surface-Enhanced Raman Scattering Anal. Chem.81
563 (2009) 2280-2285.
564 [37] J.J. Mock, M. Barbic, D.R. Smith, D.A. Schultz, S. Schultz, Shape effects in plasmon
565 resonance of individual colloidal silver nanoparticles, J. Chem. Phys. 116 (2002) 6755-6759.
566 [38] P.H.C. Eilers, Parametric Time Warping. Anal. Chem., 76 (2004) 404–411
567 [39] E.T. Whittaker, Proc. Edinburgh Math. Soc. 1923, 41, 63.
568 [40] A. Savitzky, M.J. Golay, E. Anal. Chem. 1964 36, 1627.

[41] S. Šašić, Parallel imaging of active pharmaceutical ingredients in some tablets and blends on Raman and near-infrared mapping and imaging platforms, Anal. Methods 3 (2011) 806-813.

[42] B. Vajna, I. Farkas, A. Szabó, Zs. Zsigmond, Gy. Marosi: Raman microscopic evaluation of technology dependent structural differences in tablets containing imipramine model drug, J. Pharm. Biomed. Anal., 51 (2010) 30-38.

Figure captions

Figure 1. Loadings obtained by MCR-ALS decomposition of conventional Raman chemical images of *a)* "D" tablet (prepared with dry technology) and *b)* "W" tablet (prepared with wet technology)

Figure 2. Detected API signals in conventional R-CI concentration maps of *a)* "D" tablet (dry technology) and *b)* "W" tablet (wet technology)

Figure 3. *a)* a baseline of a SERS positve spectrum estimated by Eiler's asymmetric least squares method. Comparison of SER-CI mapping spectra in *b)* raw form and after background removal using *c)* piece-wise linear baseline correction and *d)* Eiler's asymmetric least squares

Figure 4. Selected API-related MCR-ALS loadings obtained from SER-CI datasets of 'D' tablet and 'W' tablet, compared to the pure API spectrum

Figure 5. API distribution by SER-CI in randomly selected locations of 'D' and 'W' tablet

Table captions

Table 1. Number of pixels with detected API SERS signals

Table 1

Method		'D' tablet		'W' tablet	
		number of pixels with API present[1]	*% of pixels with API present*	*number of pixels with API present*[1]	*% of pixels with API present*
R-CI		*22 (961)*	*2.3%*	*9 (961)*	*0.9%*
SER-CI	Area 1	*332 (2401)*	*13.8%*	*2279 (2500)*	*91.2%*
	Area 2	*228 (2401)*	*9.5%*	*2358 (2500)*	*94.3%*
	Area 3	*245 (2401)*	*10.2%*	*2450 (2500)*	*98.0%*

[1] brackets show the overall number of pixels

Figure 1

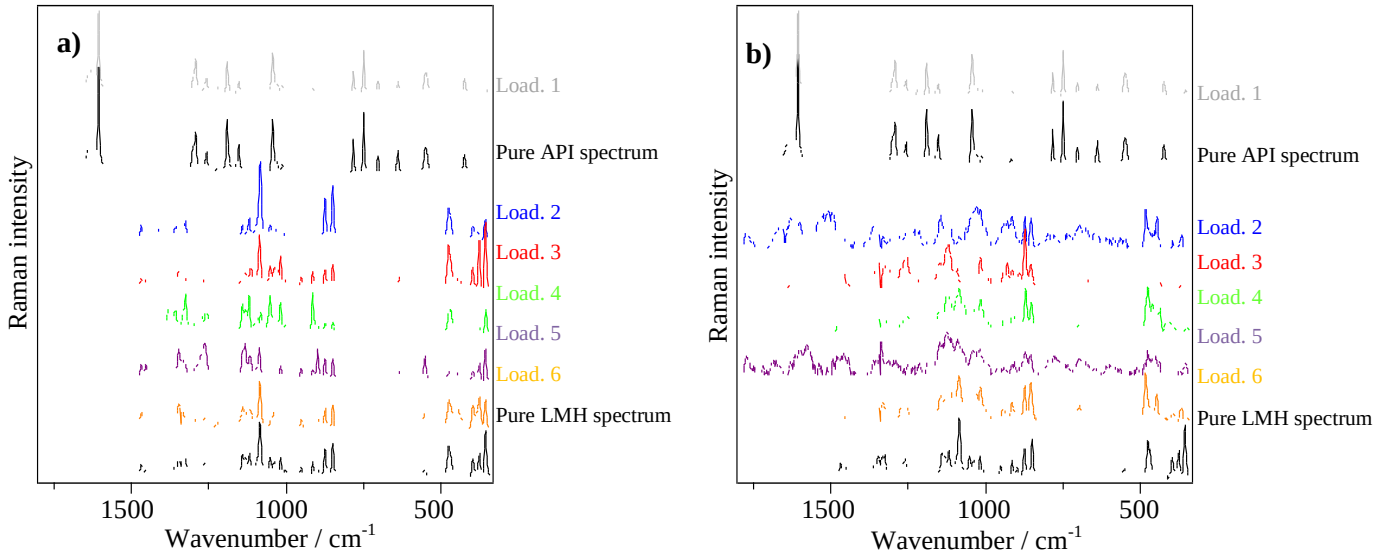
a)
b)
Raman intensity
Wavenumber / cm-1
1500
1000
500
Load. 1
Pure API spectrum
Load. 2
Load. 3
Load. 4
Load. 5
Load. 6
Pure LMH spectrum

Figure 2

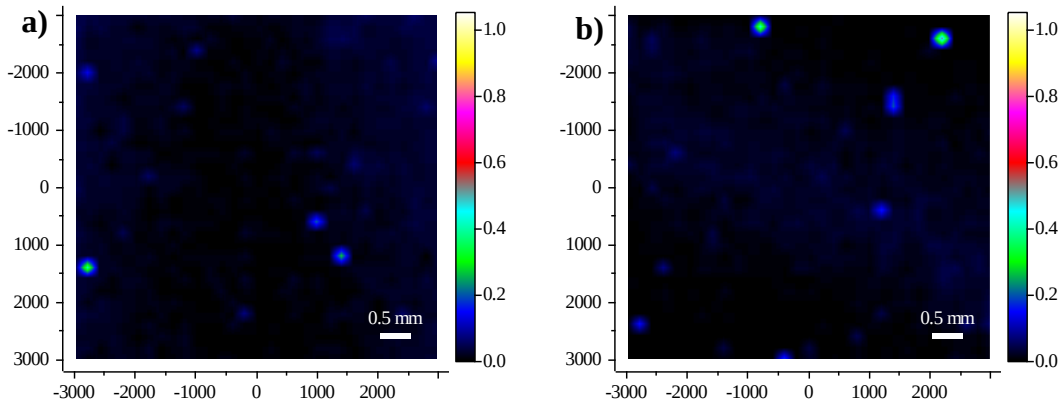

Figure 3

Click here to download high resolution image

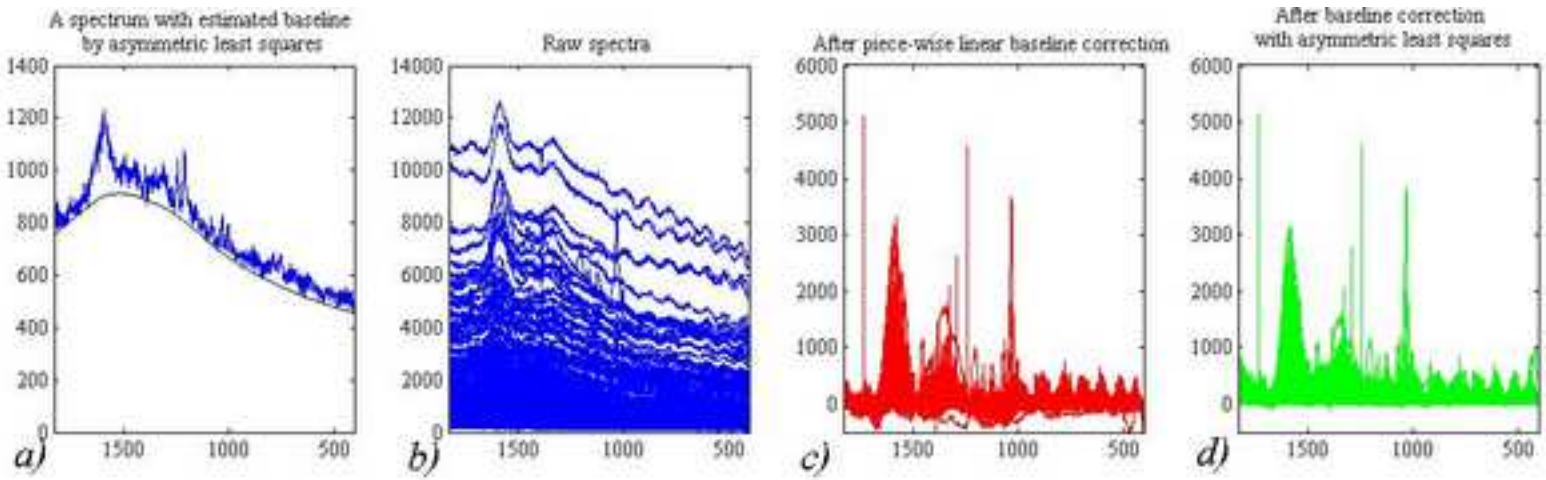

Figure 4

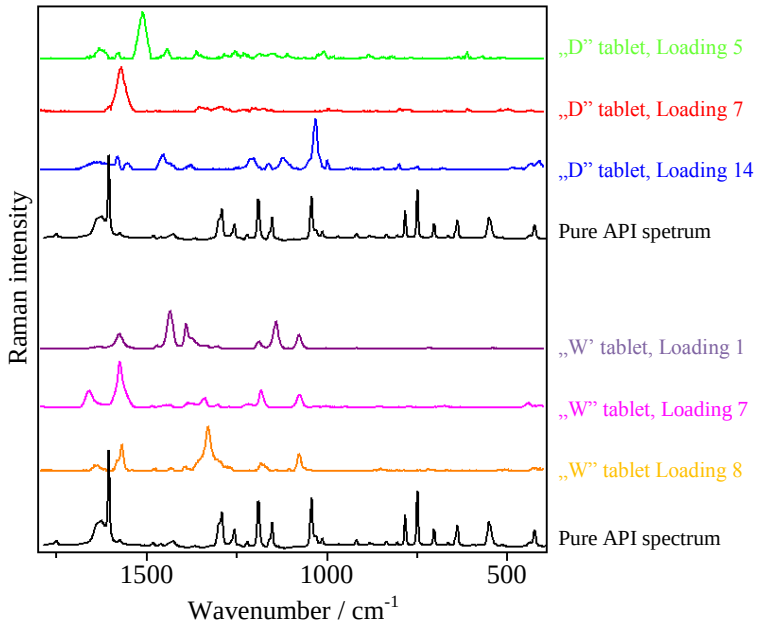
„D" tablet, Loading 5
„D" tablet, Loading 7
„D" tablet, Loading 14
Pure API spetrum
„W' tablet, Loading 1
„W" tablet, Loading 7
„W" tablet Loading 8
Pure API spectrum
Raman intensity
1500
1000
500
Wavenumber / cm-1

Figure 5